Minimax Theory and its Applications

Volume 11 (2026), No. 3s, 357 to 367

Multi-Objective Reliability–Cost Optimization of Repairable Industrial Systems under Pythagorean and Intuitionistic Fuzzy Kolmogorov Uncertainty

Sujeeta Kumari[1], Vinay Kumar[2], O. P. Sheoran[3], Sanju[4*]

[1,3]Department of Mathematics and Statistics, CCS Haryana Agricultural University, Hisar – 125004, India
Email: sujeetakaliraman@gmail.com, opsheoran1968@gmail.com
[2]Department of Statistics, Central University of Haryana, Mahendergarh-123031, Haryana, India
Email: vinay.stat@gmail.com
[4]Department of Statistics& Data Science, Maharshi Dayanand University, Rohtak-124001, India
*Corresponding author's Email: sanjukularia111@gmail.com

Abstract
This study presents a comparative optimization methodology for repairable industrial systems subject to generalized fuzzy uncertainty. We incorporate Pythagorean fuzzy sets (PFS) into dynamic Markov availability models and evaluate their behavior alongside standard intuitionistic fuzzy sets (IFS). The quadratic boundary of PFS expands non-membership supports by approximately 28% relative to the linear IFS boundary. This geometric expansion produces more conservative availability estimates, which accurately mirror epistemic ambiguity in operational failure and repair records. Three metaheuristic algorithms—multi-objective particle swarm optimization with an external repository (MOPSO), non-dominated sorting genetic algorithm II (NSGA-II), and decomposition-based evolutionary optimization (MOEA/D)—are tested on two full-scale plants: a rice milling facility and a thermal power station. Both systems are modeled through Kolmogorov differential systems coupled with time-dependent Weibull failure hazards. The optimization problem simultaneously maximizes steady-state availability and minimizes lifecycle maintenance expenses while satisfying operational availability thresholds. Across five independent random seeds, MOPSO achieves superior hypervolume values (112,640 for the rice mill and 399,893 for the thermal plant) and the lowest inverted generational distance, whereas NSGA-II exhibits uniform solution spread. Transitioning from IFS to PFS shifts Pareto frontiers toward lower availability and higher maintenance expenditure. Time-dependent Weibull hazards reduce knee-point availability by 5% to 7% compared to constant-rate models. These findings emphasize the practical necessity of accounting for component aging and broader non-membership margins during system planning.

Keywords: Pythagorean fuzzy sets; Intuitionistic fuzzy sets; Multi-objective optimization; Particle swarm optimization; NSGA-II; MOEA/D; Kolmogorov differential equations; Weibull hazard; System availability; Maintenance cost.

1. Introduction

Continuous operation in production lines and power generation plants depends heavily on component reliability and repair responsiveness. In industrial practice, unforeseen breakdowns cause costly production losses and safety risks. Plant engineers therefore seek optimal design configurations that balance high operational availability against capital and maintenance expenses. Finding this balance requires dependable mathematical models.

Classical reliability models generally treat failure and repair parameters as deterministic constants. However, empirical failure records are often limited, noisy, or gathered under varying operating conditions. Parameter estimations thus contain significant epistemic uncertainty. Fuzzy set theory provides a systematic mathematical medium for addressing such ambiguity. Atanassov extended classical fuzzy logic by formulating intuitionistic fuzzy sets (IFS), where each element carries both a membership grade μ and a non-membership grade ν under the linear restriction $\mu + \nu \leq 1$. The residual quantity represents hesitation, which distinguishes active opposition from simple lack of knowledge.

Despite its utility, the linear IFS restriction becomes restrictive when subject matter experts express substantial confidence and substantial doubt simultaneously. Yager resolved this constraint by introducing Pythagorean

fuzzy sets (PFS), which satisfy the quadratic condition $\mu^2 + \nu^2 \leq 1$. In the (μ, ν) plane, this relaxation changes the admissible domain from an orthogonal triangle into a quarter-circle. PFS accommodates coordinate pairs such as $(0.7,0.7)$ that violate IFS rules. This added flexibility is valuable when modeling conflicting expert opinions or sparse maintenance records.

Most fuzzy reliability optimization studies rely on static algebraic expressions. Dynamic Markov systems governed by Kolmogorov differential equations remain rarely integrated into multi-objective search loops under generalized fuzzy uncertainty. We address this gap by establishing an optimization pipeline that connects Pythagorean and intuitionistic fuzzy Kolmogorov solvers directly with multi-objective metaheuristics.

We evaluate three distinct algorithmic paradigms: MOPSO (swarm intelligence with repository filtering), NSGA-II (Pareto ranking with crowding distance), and MOEA/D (subproblem decomposition with Tchebycheff aggregation). To examine cross-domain consistency, the optimization is applied to two distinct industrial architectures: a rice mill processing unit and a thermal power generating station. Both systems include cold standby redundancy in their primary subsystem.

The primary contributions of this paper are:

1. Integration of Pythagorean fuzzy sets into dynamic Kolmogorov availability models, utilizing triangular Pythagorean fuzzy numbers (TPFNs) that admit roughly 28% wider non-membership supports than conventional TIFNs.
2. Systematic performance benchmarking of MOPSO, NSGA-II, and MOEA/D using hypervolume, inverted generational distance, and spread metrics across multiple random seeds.
3. Application to two separate industrial systems, verifying that algorithmic rankings and fuzzy sensitivity trends hold across different physical scales.
4. Parametric sensitivity analysis evaluating the effects of membership confidence cuts (α^*), non-membership margins (β^*), and time-dependent Weibull aging relative to constant failure rates.

2. Mathematical Formulations

2.1. Intuitionistic Fuzzy Numbers

An intuitionistic fuzzy set A over a discourse domain X is defined by a membership function $\mu_A(x)$ and a non-membership function $\nu_A(x)$ satisfying $0 \leq \mu_A(x) + \nu_A(x) \leq 1$ for all $x \in X$. The hesitation margin is $\pi_A(x) = 1 - \mu_A(x) - \nu_A(x)$. A triangular intuitionistic fuzzy number (TIFN) is represented by base triplets (a_1, a_2, a_3) for membership and (a_1', a_2, a_3') for non-membership, where $a_1' \leq a_1 \leq a_2 \leq a_3 \leq a_3'$.

For a chosen confidence cut $\alpha^* \in [0,1]$, the membership interval is given by:

$$A_{\alpha^*} = [a_1 + \alpha^*(a_2 - a_1), a_3 - \alpha^*(a_3 - a_2)]$$

For the non-membership grade $\beta^* \in [0,1]$, the conjugate cut yields:

$$A_{\beta^*} = [a_2 - \beta^*(a_2 - a_1'), a_2 + \beta^*(a_3' - a_2)]$$

In our formulation, $\alpha^* = 0$ yields the widest membership uncertainty interval, while $\alpha^* = 1$ recovers the modal value. For non-membership, $\beta^* = 0$ represents the mode and $\beta^* = 1$ yields the broadest non-membership interval.

2.2. Pythagorean Fuzzy Numbers and Support Expansion

A Pythagorean fuzzy set relaxes the linear condition to a quadratic sum, $0 \leq \mu_A(x)^2 + \nu_A(x)^2 \leq 1$. The allowable non-membership grade for a given membership value expands from $\nu \leq 1 - \mu$to $\nu \leq \sqrt{1 - \mu^2}$.

A triangular Pythagorean fuzzy number (TPFN) shares the modal core a_2 with its IFS counterpart but permits wider non-membership boundaries $[a_1', a_3']$. For a base IFS non-membership spread $s = a_2 - a_1'$, the corresponding PFS spread s' scales proportionally to the geometric boundary ratio:

$$s' = s \cdot \sqrt{\frac{1 + \nu_{max}}{1 - \nu_{max}}}$$

For representative baseline uncertainty levels, this geometric property yields approximately 28% wider non-membership support. Wider bounds widen the search space for potential parameter deviations. When propagated through the differential availability model, these expanded bounds generate lower, more conservative availability projections.

2.3. Dynamic Markov Systems and Kolmogorov Equations

Let a repairable industrial system contain N discrete states. The operational states form a working subset $W \subset \{0,1,\dots,N-1\}$. State probabilities $P(t) = [P_0(t), P_1(t), \dots, P_{N-1}(t)]^T$ evolve according to the linear differential system:

$$\frac{dP(t)}{dt} = Q(t)P(t), \qquad P(0) = [1,0,\dots,0]^T$$

Here, $Q(t)$ represents the $N \times N$ transition rate matrix. Off-diagonal elements $q_{ij}(t)$ denote transition rates from state j to state i, and diagonal entries satisfy $q_{jj}(t) = -\sum_{i \neq j} q_{ij}(t)$. The system availability at mission horizon T is:

$$A(T) = \sum_{j \in W} P_j(T)$$

The mission time is set to $T = 8760$ hours, representing one continuous operational year.

2.4. Weibull Failure Hazard Functions

Mechanical components degrade over time due to wear, thermal stress, and fatigue. We describe failure behavior using time-dependent Weibull hazard rates:

$$h(t) = \left(\frac{k}{\lambda}\right)\left(\frac{t}{\lambda}\right)^{k-1}$$

where$\lambda > 0$ is the characteristic scale parameter and $k > 0$ is the shape parameter. When $k = 1$, the failure hazard remains constant. For $k > 1$, the failure rate increases monotonically with operating hours. Under fuzzy uncertainty, parameters λ and k are defined as TIFNs or TPFNs. At each confidence cut, the certified lower availability envelope is evaluated by selecting the parameter corner that maximizes failure hazards across the time horizon.

3. System Descriptions

3.1. Rice Mill Processing Unit

The rice processing line comprises three main functional stages in series: a husking subsystem (Subsystem 1) equipped with an active unit and cold standby units, a separator (Subsystem 2), and a polishing unit (Subsystem 3). Switchover to a standby husker succeeds with coverage probability c. If switchover fails, the system transitions directly into an unavailable state.

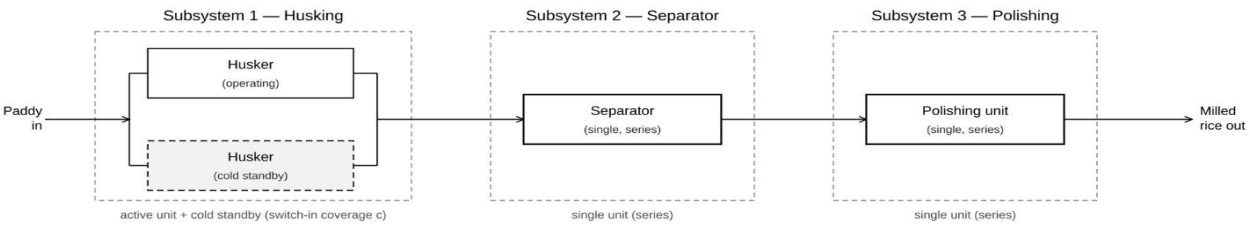


Fig. 1: Reliability Block diagram of Rice Mill Processing Unit

Fixed parameters: Husker repair rate $\mu_{fixed} = 0.020\ h^{-1}$.

Fuzzy Weibull scale parameters: $\lambda_1 = (3800,4000,4400)$, $\lambda_3 = (2800,3000,3400)$, $\lambda_4 = (1800,2000,2400)$ hours.

Fuzzy Weibull shape parameters: $k_1 = k_3 = k_4 = (1.30,1.50,1.70)$.

Cost constants: $C_S = 2 \times 10^4$, $C_R = 10^7$, $\gamma = 1.5$, $C_C = 5 \times 10^3$, $\delta = 1.2$.

Design vector: $x = (c, \mu_3, \mu_4, n_s)$, with operational bounds $c \in [0.70,0.95]$, $\mu_3 \in [0.020,0.050]\ h^{-1}$, $\mu_4 \in [0.008,0.020]\ h^{-1}$, and $n_s \in \{1,2\}$.

Availability threshold: $A_{min} = 0.70$.

3.2. Thermal Power Plant

The thermal power generation system shares a series-parallel topology with the milling plant but features distinct parameter scales. The primary stage is a steam turbine (Subsystem 1) with cold standby capacity, followed in series by a condensing system (Subsystem 2) and an electrical generator (Subsystem 3).

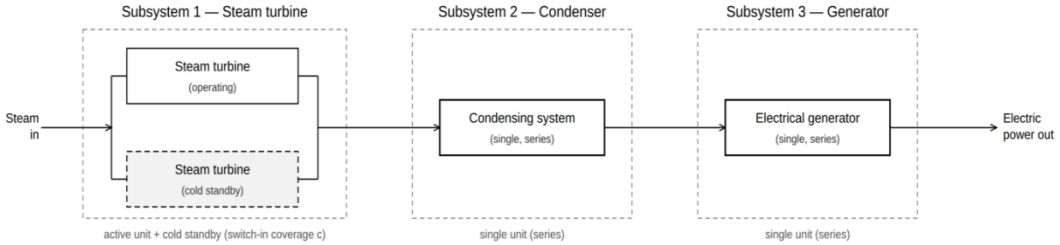


Fig. 2: Reliability block diagram of Thermal Power Plant

Fixed parameters: Turbine repair rate $\mu_{fixed} = 0.015\ h^{-1}$.

Fuzzy Weibull scale parameters: $\lambda_1 = (4500,5000,5500)$, $\lambda_3 = (3500,4000,4500)$, $\lambda_4 = (5500,6000,6500)$ hours.

Fuzzy Weibull shape parameters: $k_1 = (1.40,1.60,1.80)$, $k_3 = (1.20,1.40,1.60)$, $k_4 = (1.30,1.50,1.70)$.

Cost constants: $C_S = 5 \times 10^4$, $C_R = 2 \times 10^7$, $\gamma = 1.5$, $C_C = 8 \times 10^3$, $\delta = 1.3$.

Design vector: $x = (c, \mu_3, \mu_4, n_s)$, with bounds $c \in [0.65,0.95]$, $\mu_3 \in [0.015,0.045]\ h^{-1}$, $\mu_4 \in [0.010,0.025]\ h^{-1}$, and $n_s \in \{1,2\}$.

Availability threshold: $A_{min} = 0.65$.

4. Optimization Problem Formulation

4.1. State-Space Configuration

With n_s cold standby units, the system state space contains working states $W = \{0,1,\dots,n_s\}$, where index j denotes the number of standby units currently undergoing repair. Failure states encompass separator breakdowns ($n_s + 1$ states), polisher breakdowns ($n_s + 1$ states), coverage switch failures (n_s states), and complete primary stage exhaustion (1 state). The total state count is exactly $N = 4(n_s + 1)$.

To accelerate search evaluations, the time-dependent transition rate matrix $Q(t)$ is separated into structural matrices:

$$Q(t) = h_1(t)B_1 + h_3(t)B_3 + h_4(t)B_4 + F$$

Matrices B_1, B_3, and B_4 encode failure transitions for the three respective stages, while F captures state repairs. This decomposition allows vectorized Runge-Kutta numerical integration across entire candidate swarms simultaneously.

4.2. Maintenance Cost Function

Total capital and maintenance cost combines standby hardware investment, repair staffing, and switching coverage technology:

$$C(x) = C_S \cdot n_s + C_R \cdot (\mu_3^\gamma + \mu_4^\gamma) + C_C \cdot \left(\frac{c}{1-c}\right)^\delta$$

The exponent $\gamma = 1.5$ introduces nonlinear penalties for high repair speeds. The coverage term exhibits an asymptotic increase as c approaches unity, reflecting steep technological expenses needed for near-perfect automatic switching.

4.3. Bi-Objective Model and Constraints

The optimization problem is formulated as:

$$\max_{x \in \Omega} \quad A_{cert}(x; \alpha^*) \qquad \text{and} \qquad \min_{x \in \Omega} \quad C(x)$$

subject to:

$$A_{cert}(x; \alpha^*) \geq A_{min}, \qquad x \in \Omega$$

whereΩ defines the hyperbox of bounded design variables. Constraint violations are handled using an exterior penalty factor of $10^6 \cdot (A_{min} - A_{cert})$.

5. Multi-Objective Optimization Algorithms

5.1. Multi-Objective Particle Swarm Optimization (MOPSO)

MOPSO guides candidate particles using cognitive memory and non-dominated leaders selected from an external archive. Velocity and position updates follow:

$$v_i(k+1) = w(k)v_i(k) + c_1 r_1 (p_i^{best} - x_i(k)) + c_2 r_2 (g^{best} - x_i(k))$$

$$x_i(k+1) = x_i(k) + v_i(k+1)$$

The inertia weight $w(k)$ decreases linearly from 0.9 to 0.4 over K_{max} iterations:

$$w(k) = 0.9 - 0.5\left(\frac{k}{K_{max} - 1}\right)$$

Acceleration constants are set to $c_1 = c_2 = 2.0$. The global guide g^{best} is selected from the external repository using roulette wheel sampling weighted by crowding distance.

5.2. NSGA-II and MOEA/D Algorithms

NSGA-II maintains population diversity through non-dominated sorting and crowding distance comparisons. Offspring solutions are produced via simulated binary crossover (SBX, distribution index $\eta_c = 20$) and polynomial mutation ($\eta_m = 20$, mutation probability $p_m = 0.25$).

MOEA/D decomposes the bi-objective space into scalar subproblems using uniformly spaced weight vectors w_j along the unit simplex. Each subproblem minimizes the Tchebycheff distance to the reference point z^*:

$$g^{tch}(x \mid w_j, z^*) = \max_{m \in \{1,2\}} \{w_{j,m} \cdot |f_m(x) - z_m^*|\}$$

Each subproblem interacts with a local neighborhood of size $T_n = 10$.

5.3. Algorithmic Control Settings

All three metaheuristics operate with a population size of 50 for 100 generations across 5 independent random seeds. Numerical ODE integration uses a step size of $h = 20$ hours during exploratory search and $h = 1.0$ hour for final Pareto re-evaluation. Standby units n_s are mapped to integer values via standard rounding.

6. Numerical Results and Discussion

6.1. Algorithmic Performance Comparison

The non-dominated trade-off frontiers obtained by MOPSO, NSGA-II, and MOEA/D at the widest membership confidence cut ($\alpha^* = 0$) underWeibull failure hazards are shown in Figures 1 and 2. MOPSO and NSGA-II produce continuous and well-populated frontiers. In contrast, MOEA/D exhibits gaps in the high-cost domain. Table 1 summarizes the corresponding knee points.

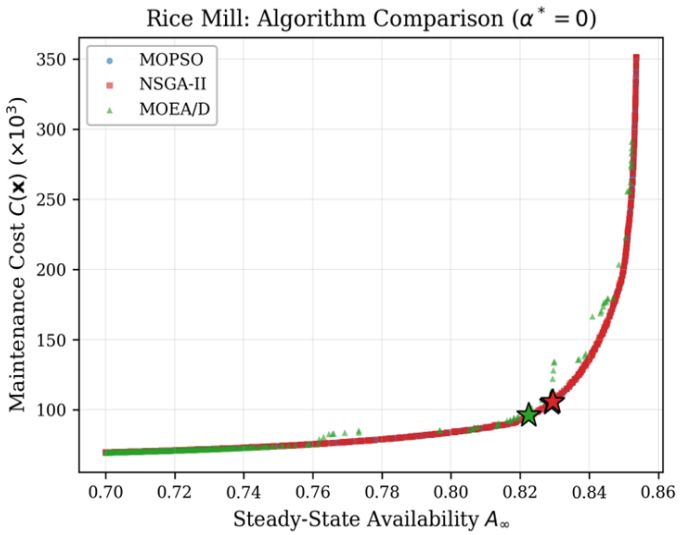


Fig. 3: Rice mill processing plant: Pareto-optimal trade-off frontiers generated by MOPSO, NSGA-II, and MOEA/D at $\alpha^* = 0$ (Weibull hazard, IFS). Stars denote identified knee points.

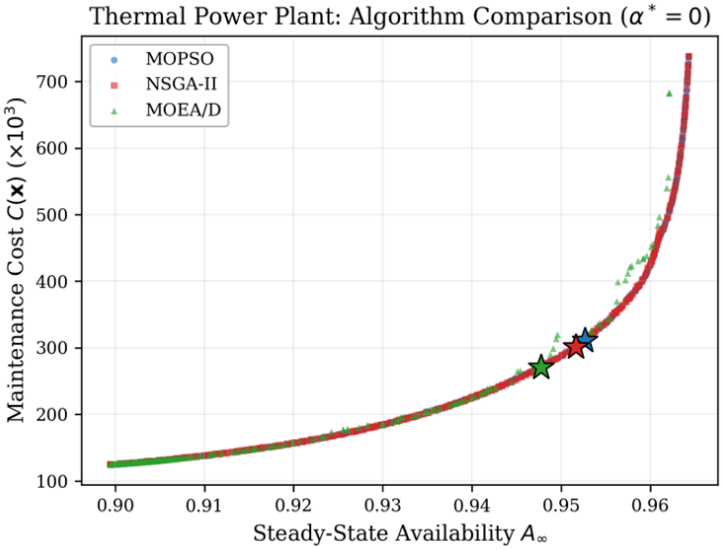


Fig. 4: Thermal power generation plant: Pareto-optimal trade-off frontiers generated by MOPSO, NSGA-II, and MOEA/D at $\alpha^* = 0$ (Weibull hazard, IFS). Stars denote identified knee points.

Table 1: Knee-point solutions across optimization algorithms ($\alpha^* = 0$, Weibull hazard, IFS).

Algorithm	A_∞(Rice Mill)	Cost$\times 10^3$(Rice Mill)	A_∞(Thermal)	Cost$\times 10^3$(Thermal)
MOPSO	0.8290	104.9	0.9527	311.2
NSGA-II	0.8294	105.6	0.9517	301.5
MOEA/D	0.8224	96.1	0.9478	270.6

For the rice milling plant, MOPSO and NSGA-II reach nearly identical knee points ($A_\infty \approx 0.829$, Cost $\approx 105 \times 10^3$). MOEA/D produces a lower availability balance ($A_\infty = 0.8224$, Cost $= 96.1 \times 10^3$). In the thermal power system, MOPSO achieves the highest knee availability of 0.9527 at a cost of 311.2×10^3.

6.2. Sensitivity to Membership Confidence Level (α^*-Cuts)

The choice of confidence level α^* directly alters the certified lower availability envelope. Figures 3 and 4 show the sensitivity of the Pareto front to α^* for the rice mill and thermal power plant respectively. Table 2 details the knee-point positions across three confidence cuts.

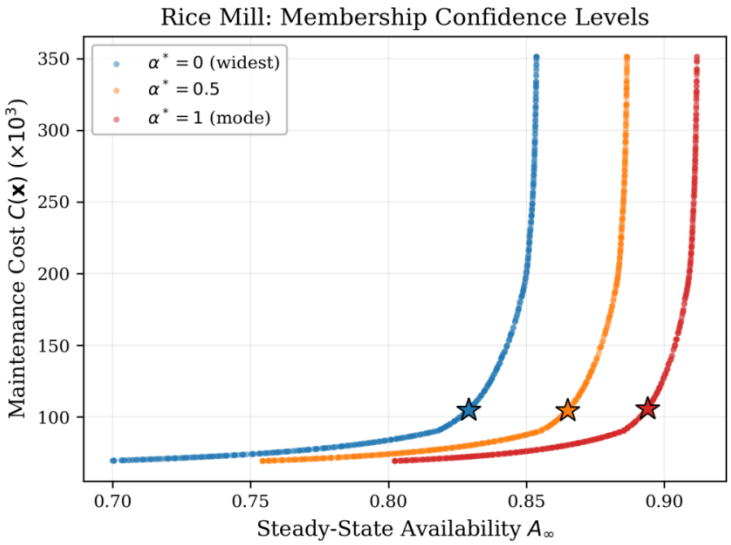


Fig. 5: Rice mill processing plant: Shift in the MOPSO Pareto frontier across membership confidence levels $\alpha^* \in \{0.0, 0.5, 1.0\}$ under Weibull failure hazards.

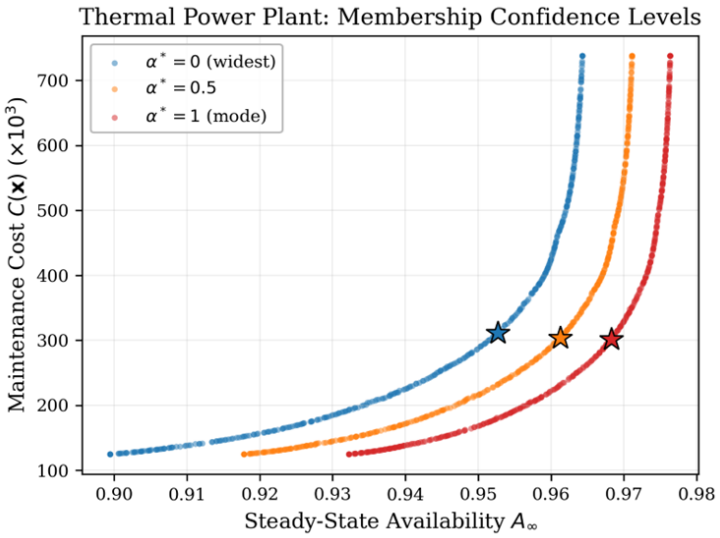


Fig. 6: Thermal power generation plant: Shift in the MOPSO Pareto frontier across membership confidence levels $\alpha^* \in \{0.0, 0.5, 1.0\}$ under Weibull failure hazards.

Table 2: Knee-point availability and maintenance expenditure at varying α^*-cuts (MOPSO, Weibull, IFS).

α^*Level	**A_∞(RM)**	**Cost$\times 10^3$(RM)**	**|PF|(RM)**	**A_∞(TP)**	**Cost$\times 10^3$(TP)**	**|PF|(TP)**
0.0 (Worst-case)	0.8290	104.9	474	0.9527	311.2	393
0.5 (Intermediate)	0.8648	104.5	472	0.9612	303.5	412
1.0 (Modal / Crisp)	0.8938	106.0	466	0.9683	301.3	405

Tightening the confidence requirement from $\alpha^* = 1.0$ down to $\alpha^* = 0.0$ reduces knee availability by 7.8% in the rice mill (from 0.8938 to 0.8290) and by 1.6% in the thermal plant (from 0.9683 to 0.9527). The cost remains relatively stable around 105×10^3 and 305×10^3 respectively. The drop in availability quantifies the safety margin needed against parametric drift.

6.3. Time-Dependent Weibull vs. Constant Failure Rates

Figure 5 compares Pareto frontiers obtained under time-dependent Weibull aging against constant failure rates evaluated at the midpoint $t = 4380$ hours. Table 3 details the corresponding numerical comparisons.

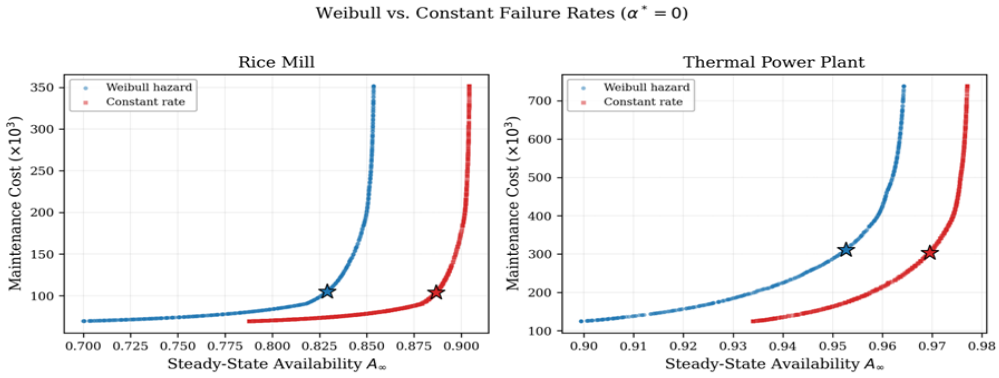


Fig. 7: Comparison of Pareto frontiers obtained under time-dependent Weibull aging versus constant failure rates at $\alpha^* = 0$ (MOPSO, IFS) for both the rice mill and thermal power plant.

Table 3: Knee-point comparison between Weibull hazard and constant failure rates (MOPSO, $\alpha^* = 0$, IFS).

Hazard Formulation	A_∞ (Rice Mill)	Cost$\times 10^3$(Rice Mill)	A_∞(Thermal)	Cost$\times 10^3$(Thermal)
Weibull Aging ($k > 1$)	0.8290	104.9	0.9527	311.2
Constant Failure Rate	0.8867	103.7	0.9695	303.7

Assuming constant failure rates overestimates availability by 7.0% in the rice mill and by 1.8% in the thermal station. Constant rates ignore wear-out accumulation. Time-dependent models prevent overly optimistic availability forecasts in aging machinery.

6.4. Comparative Analysis: Intuitionistic vs. Pythagorean Uncertainty

Figure 6 illustrates the Pareto-optimal frontiers under intuitionistic versus Pythagorean fuzzy uncertainty at the maximum non-membership margin ($\beta^* = 1.0$). Table 4 reports the numerical knee points.

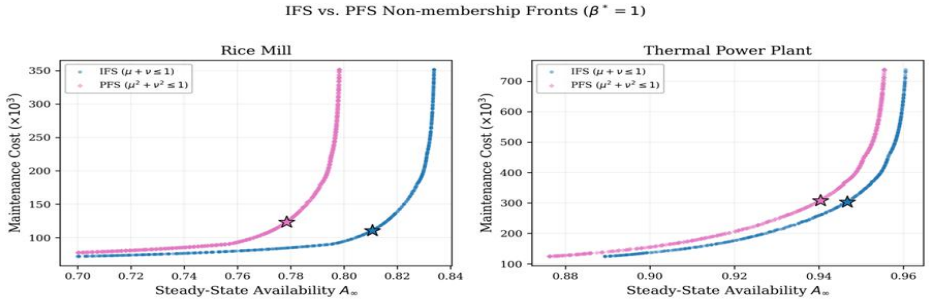


Fig. 8: Comparison of intuitionistic fuzzy (IFS) and Pythagorean fuzzy (PFS) non-membership Pareto frontiers at $\beta^* = 1.0$ (MOPSO, Weibull hazard) for both industrial systems.

Table 4: Knee-point comparison under IFS and PFS non-membership conditions ($\beta^* = 1.0$, MOPSO, Weibull).

Uncertainty Model	A_∞(Rice Mill)	Cost$\times 10^3$(Rice Mill)	A_∞(Thermal)	Cost$\times 10^3$(Thermal)
IFS ($\mu + \nu \leq 1$)	0.8106	110.7	0.9467	303.5
PFS ($\mu^2 + \nu^2 \leq 1$)	0.7785	123.3	0.9404	308.5

Pythagorean fuzzy sets shift the Pareto frontier toward lower availability and higher maintenance cost. For the rice processing unit, knee availability drops by 3.96% (0.7785 versus 0.8106), while cost rises by 11.4% (123.3×10^3 versus 110.7×10^3). In the thermal facility, availability decreases by 0.67% and expenditure increases by 1.6%.

This shift stems from the expanded non-membership boundaries in PFS. The wider interval encompasses more severe degradation scenarios. When maintenance data involves significant expert dispute, PFS prevents underestimating required repair resources.

6.5. Quantitative Quality Indicators and Convergence

Figure 7 displays the hypervolume convergence trajectories across 100 generations, while Figure 8 illustrates the metric distributions over five independent random seeds. Table 5 summarizes the numerical results.

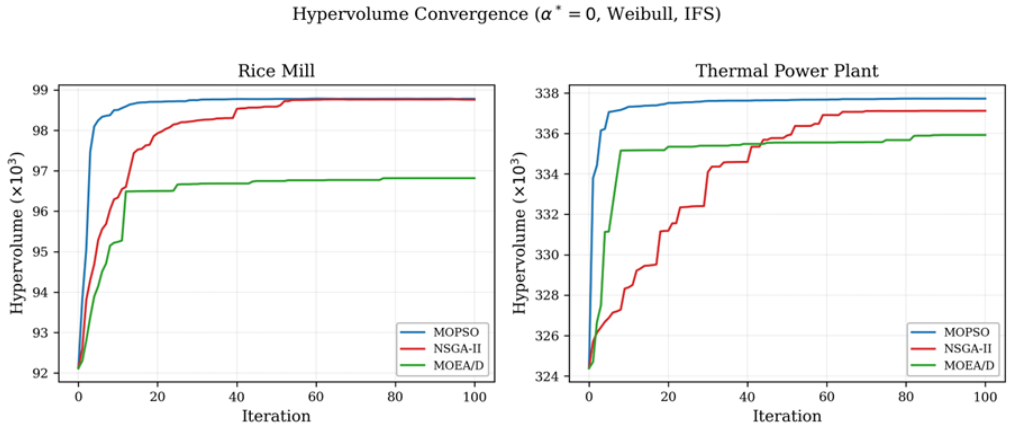


Fig. 9: Hypervolume metric convergence trajectories over 100 iterations for MOPSO, NSGA-II, and MOEA/D ($\alpha^* = 0$, Weibull hazard, IFS, seed 0).

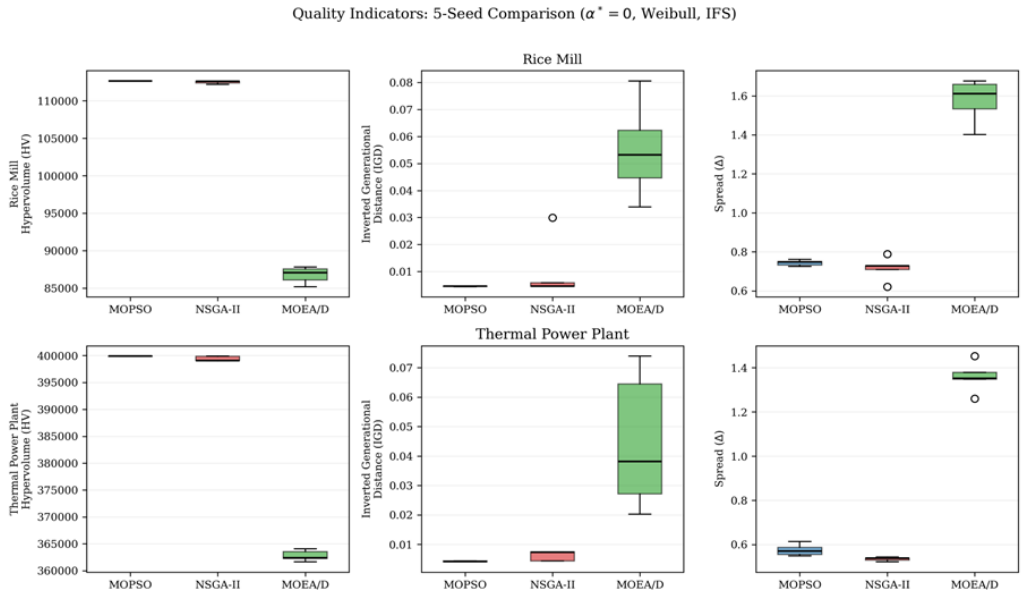


Fig. 10: Performance indicator distributions across five independent random seeds: Hypervolume (higher is better), Inverted Generational Distance (lower is better), and Spread (lower is better).

Table 5: Performance metrics across five independent seed runs (mean ± standard deviation).

System	Algorithm	Hypervolume (HV)	Pareto Size |PF|	Inverted Gen. Dist. (IGD)	Spread (Δ)
Rice Mill	MOPSO	112,640 ± 4	474	0.0045 ± 0.0001	0.744 ± 0.013

Rice Mill	NSGA-II	$112{,}479 \pm 180$	387	0.0099 ± 0.0100	0.715 ± 0.054
Rice Mill	MOEA/D	$86{,}757 \pm 973$	416	0.0549 ± 0.0159	1.576 ± 0.101
Thermal Plant	MOPSO	$399{,}893 \pm 4$	393	0.0043 ± 0.0001	0.575 ± 0.023
Thermal Plant	NSGA-II	$399{,}391 \pm 408$	328	0.0062 ± 0.0015	0.535 ± 0.008
Thermal Plant	MOEA/D	$362{,}785 \pm 891$	307	0.0448 ± 0.0209	1.358 ± 0.061

MOPSO achieves the highest hypervolume and lowest IGD on both systems with small variance (HV std = 4). NSGA-II provides competitive convergence and the best spread values (0.715 for the rice mill, 0.535 for the thermal plant). MOEA/D records 10% to 23% lower hypervolume and higher IGD values due to non-uniform weight mappings.

6.6. Optimal Decision Variable Selection

Table 6 lists the decision variables corresponding to the knee points.

Table 6: Optimal decision variable configurations at Pareto knee points ($\alpha^* = 0$, Weibull, IFS).

System	Algorithm	Coverage c	Repair μ_3 (h^{-1})	Repair μ_4 (h^{-1})	Standby Units n_s
Rice Mill	MOPSO	0.7000	0.02638	0.02000	1
Rice Mill	NSGA-II	0.7000	0.02666	0.02000	1
Rice Mill	MOEA/D	0.7076	0.02250	0.01984	1
Thermal Plant	MOPSO	0.7999	0.03548	0.02500	1
Thermal Plant	NSGA-II	0.7892	0.03446	0.02500	1
Thermal Plant	MOEA/D	0.7736	0.02995	0.02465	1

All knee solutions select a single cold standby unit ($n_s = 1$). Adding a second standby unit incurs high capital costs that yield minor availability increments. Coverage factors stay near lower practical boundaries ($c = 0.70$ in the rice mill, $c \approx 0.78$–0.80 in the thermal plant). Repair rates remain moderate, balancing infrastructure expenditure against downtime penalties.

7. Conclusions

This study evaluated multi-objective reliability-cost optimization for repairable industrial systems under intuitionistic and Pythagorean fuzzy uncertainty. The main conclusions are:

1. Incorporating Pythagorean fuzzy sets expands non-membership supports by approximately 28% compared to intuitionistic models. This expansion shifts the Pareto frontier toward lower availability and higher maintenance expenditure, reducing knee availability by 3.96% in the rice mill and by 0.67% in the thermal plant. This shift measures the cost of accommodating broader epistemic uncertainty.
2. MOPSO demonstrates the strongest overall convergence, achieving the highest hypervolume and lowest inverted generational distance across both test systems with minimal variance. NSGA-II delivers competitive hypervolume alongside superior front uniformity, while standard MOEA/D requires adaptive weight adjustment for stiff ODE-constrained surfaces.
3. Ignoring wear-out behavior through constant failure rates overestimates knee-point availability by up to 7.0%, demonstrating the importance of time-dependent Weibull modeling.
4. Algorithmic rankings and sensitivity responses match across both industrial case studies, confirming the broad applicability of the proposed methodology.

Future research will investigate interval-valued Pythagorean formulations, adaptive decomposition strategies, and surrogate-assisted integration schemes for larger Markov chains.

References

1. Atanassov, K. T. (1986). Intuitionistic fuzzy sets. Fuzzy Sets and Systems, 20(1), 87–96.

2. CoelloCoello, C. A., &Lechuga, M. S. (2002). MOPSO: A proposal for multiple objective particle swarm optimization. In Proceedings of the 2002 IEEE Congress on Evolutionary Computation (CEC'02) (pp. 1051–1056). Honolulu, HI, USA.

3. Deb, K., Pratap, A., Agarwal, S., &Meyarivan, T. (2002). A fast and elitist multiobjective genetic algorithm: NSGA-II. IEEE Transactions on Evolutionary Computation, 6(2), 182–197.

4. Gen, M., & Cheng, R. (1999). Genetic algorithms and engineering optimization. John Wiley & Sons.

5. Kumar, A., Singh, S. B., & Ram, M. (2019). Reliability optimization of complex systems using Markov chain and particle swarm optimization. International Journal of System Assurance Engineering and Management, 10(5), 1285–1296.

6. Li, D. F. (2010). A ratio ranking method of triangular intuitionistic fuzzy numbers and its application to MADM problems. Computers & Mathematics with Applications, 60(6), 1557–1570.

7. Peng, X., & Yang, Y. (2015). Some results for Pythagorean fuzzy sets. International Journal of Intelligent Systems, 30(11), 1133–1160.

8. Shi, Y., &Eberhart, R. C. (1998). A modified particle swarm optimizer. In Proceedings of the IEEE International Conference on Evolutionary Computation (ICEC'98) (pp. 69–73). Anchorage, AK, USA.

9. Weibull, W. (1951). A statistical distribution function of wide applicability. Journal of Applied Mechanics, 18(3), 293–297.

10. Yager, R. R. (2014). Pythagorean membership grades in multicriteria decision making. IEEE Transactions on Fuzzy Systems, 22(4), 958–965.

11. Yager, R. R., &Abbasov, A. M. (2013). Pythagorean membership grades, complex numbers, and decision making. International Journal of Intelligent Systems, 28(5), 436–452.

12. Zhang, Q., & Li, H. (2007). MOEA/D: A multiobjective evolutionary algorithm based on decomposition. IEEE Transactions on Evolutionary Computation, 11(6), 712–731.

13. Zhang, X., &Xu, Z. (2014). Extension of TOPSIS to multiple criteria decision making with Pythagorean fuzzy sets. International Journal of Intelligent Systems, 29(12), 1061–1078.

14. Zitzler, E., & Thiele, L. (1999). Multiobjective evolutionary algorithms: A comparative case study and the strength Pareto approach. IEEE Transactions on Evolutionary Computation, 3(4), 257–271.

15. Zitzler, E., Thiele, L., Laumanns, M., Fonseca, C. M., &Grunert da Fonseca, V. (2003). Performance assessment of multiobjective optimizers: An analysis and review. IEEE Transactions on Evolutionary Computation, 7(2), 117–132.